Electrical Resistivity of Izu-Oshima Volcano

Electromagnetic Research Group of Izu-Oshima Volcano*

The electrical resistivity of a rock is highly dependent on thermal conditions. When temperature rises, the resistivity decreases. If the rock melts, resistivity decreases drastically. Fluids contained in a rock also work to reduce resistivity, since fluids with high ion content are electrically conducting. The resistivity of the fluids depends also on temperature. A fluid of high temperature is usually more conducting than one of low temperature (see, for example, Keller and Frischknecht, 1966).

Because of these properties of rock resistivity, electrical resistivity surveys are common in geothermal energy exploration. Resistivity measurements are also useful in examination of the thermal structure of a volcano. During and prior to a volcanic eruption, not only the temperature but also hydrothermal system changes inside a volcano, resulting in a change in electrical resistivity. For this reason, the measurement of the resistivity of the volcano is an effective tool in monitoring its activity.

In association with the eruption in November, 1986, remarkable changes in resistivity were observed (Yukutake et al., 1987). On Oshima volcano, two techniques are used to measure resistivity. One is the direct current method, in which artificially controlled electric currents are driven into the ground and differences in the electric potential are measured to obtain the resistivity of the earth (Yukutake et al., 1983). The other is the electromagnetic induction method, in which time varying electric and magnetic fields are measured to estimate the induced fields inside the earth.

1. Resistivity changes obtained by a direct current method.

Electrode arrangements

Across the central crater electrodes are installed as shown in Fig. 1. I_1, I_2 and I_3 are current electrodes through which the electric currents are driven into the ground. V_1, V_2 and V_3 are potential electrodes between which the electrical potential differences are measured. The measurements were made for three different pairs of electrodes. In pair A, currents were driven through I_1 and I_2, and potential differences were measured between V_1 and V_2. In pair B, currents through I_1 and I_3, and potential differences between V_1 and V_3, In pair C, currents through I_2 and I_3, and potential differences between V_2 and V_3. The distances between the mid-points of the current and the potential electrodes are 750m for the electrode pair A, 950m for B, and 1150m for C.

---

*) Manuscript prepared by Takesi Yukutake, Earthquake Research Institute, University of Tokyo

Apparent resistivity

From the measurement of the potential differences, apparent resistivity (ρ_a) is first computed. Suppose the earth is homogeneous with a constant resistivity ρ_a, and bounded by a plane surface. The apparent resistivity is defined as

$$\rho_a = K \frac{\Delta V}{\Delta L} \frac{1}{I} \quad ,$$

where ΔV is the measured potential difference, ΔL the distance between the potential electrodes, I the intensity of the electric current driven into the ground and K is a geometrical factor determined by configuration of the electrodes.

The apparent resistivities obtained for the three pairs of electrodes at the time of initiation of the experiments are plotted in Fig. 2, denoted by A, B and C. The apparent resistivity increases with increase in separation distance between the current and the potential electrode pairs.

Figure 2 also shows apparent resistivities obtained by the measurements on the caldera floor. Open circles (N) are the results of the bipole-bipole arrangements of the electrodes, while solid circles are those of Schlumberger arrangements. The apparent resistivity decreases with increase in the electrode spacings. This implies that the real resistivity decreases with increase of depth.

The trend of apparent resistivity obtained by the measurement across the central crater is opposite to the general trend described above. The apparent resistivity increases with the separation distance between the electrodes. At a first glance, this appears to suggest that the resistivity increases with increase in depth. However, this is not true.

At the time of initiation of the repeated resistivity measurements, a big crater was present in the Mihara-yama cinder cone. Such an empty hole has a great influence on the distribution of the electric currents in the ground, and causes an unexpected effect on the measured apparent resistivity (Yukutake et al., 1983). The effect is to reduce the apparent resistivity obtained for the nearest pair of electrodes, A. Since the effect is negligible for the measurement with the farthest pair, C, the apparent resistivity tends to increase with the separation distance, even though no resistivity increase occurs with depth. Figure 3 shows how the apparent resistivity increases with the separation distance for a simple ellipsoidal hole in a uniform earth with a constant resistivity.

Accordingly, as magma rises, the volume of the hole diminishes. Then the apparent resistivity for measurement A is expected to increase. On the other hand, the resistivity for C is considered to reflect resistivity of deeper parts of the central cone. Therefore, if low resistivity magma rises up from depths, and heats the surrounding materials, apparent resistivity for measurement C is supposed to decrease.

Time variation in the apparent resistivity

The results of the repeated measurements are shown in Fig. 4. The values of the apparent resistivity are normalized by those of the first

measurement in March, 1975.

After repetition of small fluctuations, the apparent resistivity started to increase around July 1985 for measurement A. This implies that magma had begun to rise. Since January 1986, the rate of increase has been accelerated until the eruption on November 15. The last measurement was made on November 16, when the normalized resistivity had reached 1.17. At this time, the crater was filled with magma to a depth of about 100 m from the surface. After this measurement, electrodes and cables were destroyed by eruptions.

On the other hand, the apparent resistivity for C began to decrease in January 1986. Although it changed to an increase in March, it began to decrease again in July at much larger rate than before. On November 8, it became as low as 0.64, about 50 percent of its peak value. The rapid decrease of the apparent resistivity for C is likely related to the rise of magma.

More details of the variations are shown in Fig. 5. Although the measuring system A was destroyed after November 16, the measurement of electrode pair C has been continued. The apparent resistivity decreased to as low as 0.47 on November 18. On November 21, however, when the fissure eruption occurred, it was already on a recovery stage. When the measurement of electrode pair C was restarted on December 6, the apparent resistivity had been already recovered to the level before eruption. Since then it has decreased continuously.

2. Resistivity changes observed by induction methods

The electromagnetic induction method as well as the direct current method has been employed to investigate the resistivity change of Oshima Volcano. Electromagnetic variations of ELF (8-20 Hz) and VLF (17.4 kHz) frequency ranges are measured.

Figure 6 shows the distribution of apparent resistivity obtained by measurements of 8 Hz in October 1986, about a month before the eruption. It is apparent that a low resistivity zone extends from the central crater in a west-southwest and east-northeast direction. In August, the low resistivity zone was restricted to a small area surrounding the crater and no such extension was observed. The extension and shrinkage of the low resistivity zone is sensitively reflected in the time variation of apparent resistivity at site E841203.

Figure 7 shows the time variation. Apparent resistivity at one site is estimated from two different pairs of the electric and the magnetic field measurements. One is from the east component of the electric (E_y) and the north component of the magnetic field (H_x). The other is from the north component of the electric (E_x) and the east component of the magnetic field (H_y). The results of these different pairs are plotted by open circles for E_y/H_x and solid circles for E_x/H_y. The figure shows apparent resistivity for two frequencies, 8 Hz and 14 Hz. For both frequencies, open circles show that the apparent resistivity decreased before the eruption and recovered in the two months after the eruption. On the other hand, solid circles do not show such variations throughout the entire

period of eruptive activity. This is consistent with the expansion of the low resistivity zone approximately in an east west direction before the eruption.

3. Resistivity anomaly map

Because of the low resistivity of magma, when a time-varying electromagnetic field is applied to a dike filled with magma, strong electric currents are induced in it. The induced currents along the dike produce a magnetic field. Therefore, by measuring the magnetic field, both the vertical and the horizontal components, it is possible to locate the magma-filled dike.

A magnetic field of 17.4 kHz from an artificial source was used to explore the low resistivity zone of Oshima volcano. The vertical (Z) and the horizontal component (H) were simultaneously measured on a helicopter at an altitude of 100 m above the ground. Then the gradient of Z/H was computed and delineated (Fig. 8). There is high possibility that low resistivity materials exist below the maxima or minima of the gradient. C and B on the map approximately correspond to the fissures along which magma erupted on November 21. There are other anomaly belts, D and E, running parallel to the fissures C and B. These coincide with the location of fissures of historical eruptions. However, this does not necessarily mean that molten lava exists below these anomaly belts, because resistivity of rocks containing large amount of water is also as low as molten lava. These belts are suspected to be fracture zones with high water contents.

Anomaly areas are also present along the caldera rim inside the caldera. This is very likely to be caused by a water reservoir that is supposed to be formed along the caldera wall, since the caldera wall occasionally works as an impenetrable barrier to ground water.

There is another anomaly belt (F) running in a southeast direction from the southeastern part of the caldera rim. The cause of this anomaly is not yet known. This could be a structural boundary between fragmental materials distributed to the east of caldera and solid non-porous lava in the south. Fluids contained in the fragmental materials might cause the anomaly belt.

Even though many of the anomaly belts are not of magmatic origin but rather results from high water content, they are indicators of structurally weak zones, such as fractured zones or structural boundaries. There is a higher possibility that magma will intrude into these weak zones than in other area.

A continuously measuring system of electrical resistivity is a very useful monitoring tool, if it is set up near the places where the magma intrusion is anticipated. There seems to be a high chance of detecting precursory signs before an eruption, as in the case of the eruption of the central crater f Mihara-yama in November, 1986.

References

Keller, G. V. and F. C. Frischknecht, Electrical Methods in Geophysical Prospecting, Pergamon Press, Oxford, 1-517, 1966.

Yukutake, T., T. Yoshino, H. Utada, T. Shimomura, and E. Kimoto, Changes in the apparent resistivity of Oshima volcano observed during a period of highly elevated tectonic activity, Earthq. Predict., 2, 83-96, 1983.

Yukutake, T., T. Yoshino, H. Utada, H. Watanabe, Y. Hamano, Y. Sasai, and T. Shimomura, Changes in the electrical resistivity of the central cone, Miharayama, of Izu-Oshima volcano, associated with its eruption in November, 1986, Proc. Japan Acad., 63, Ser. B, 55-58,1987.

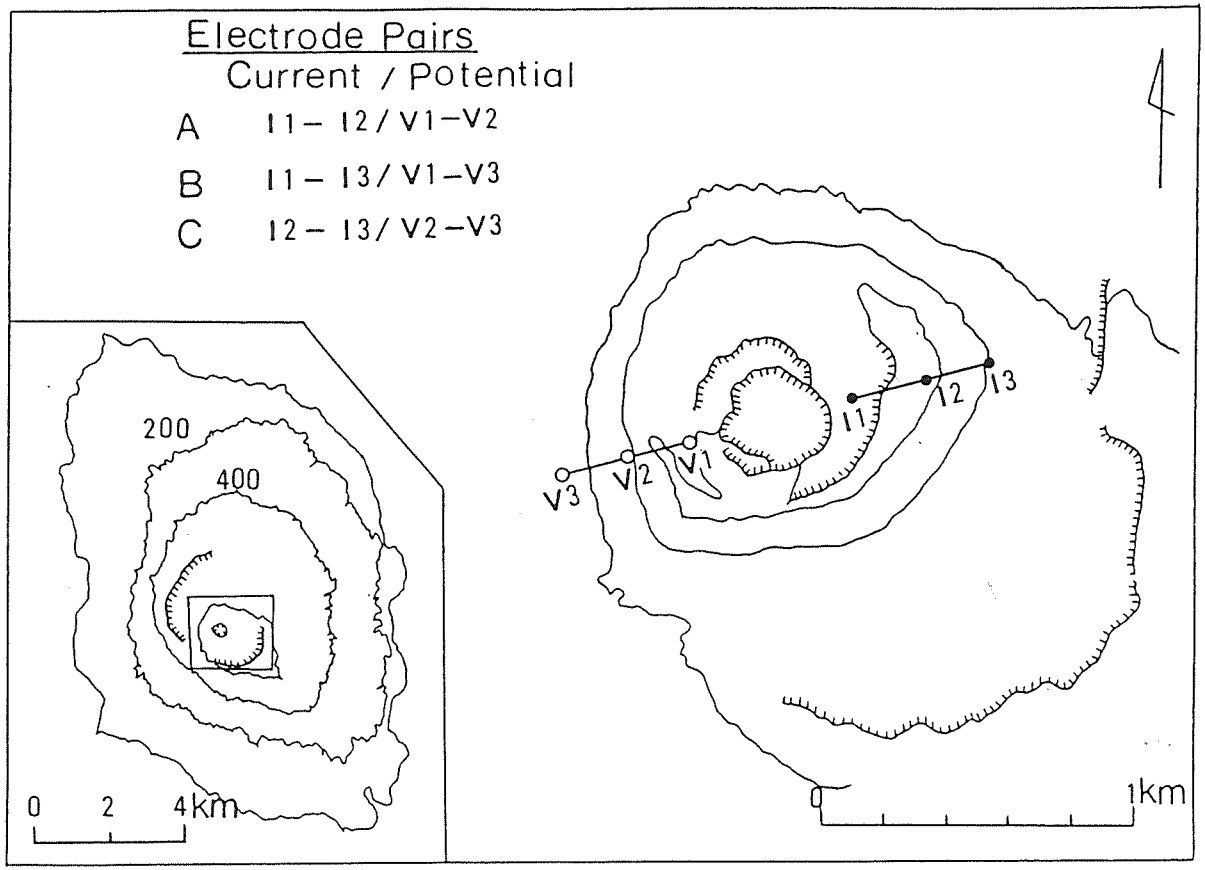

Fig. 1 Electrode arrangements across the central crater, Mihara-yama.

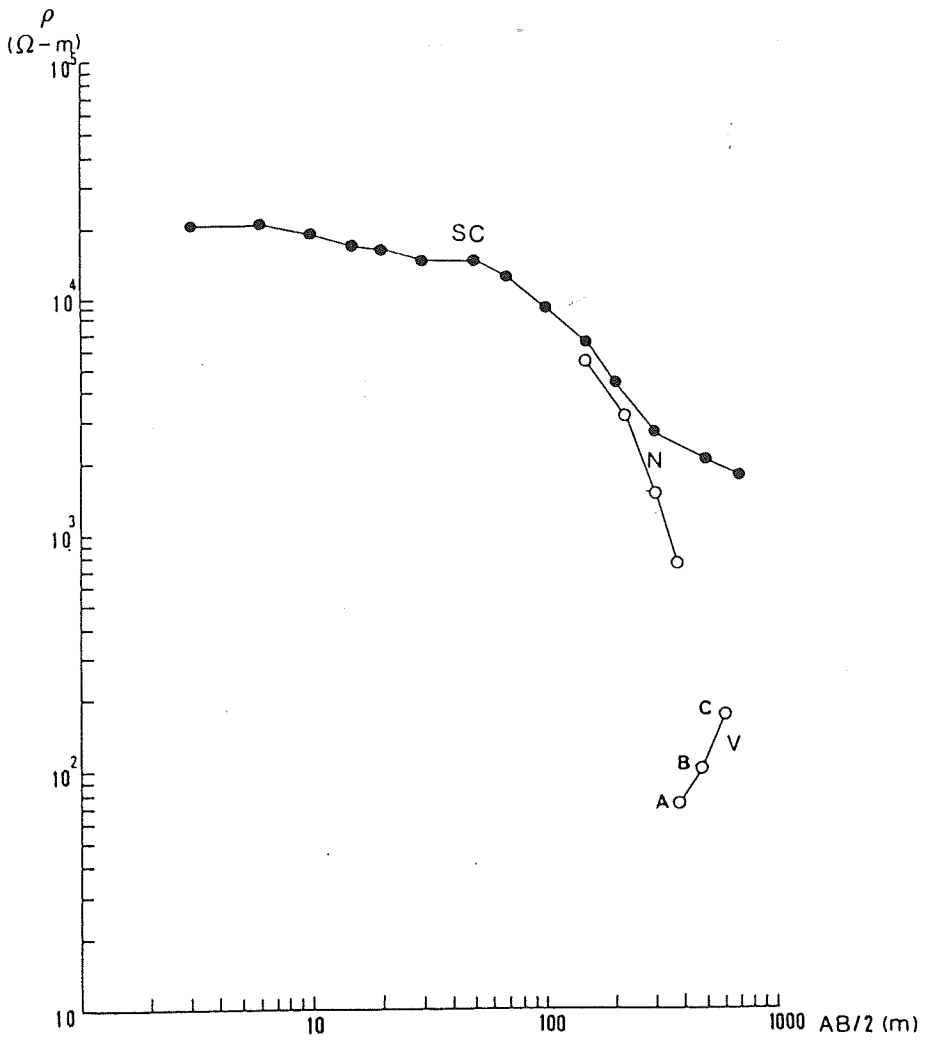

Fig. 2 Apparent resistivities obtained by direct current methods on the caldera floor and across the central crater. Solid circles are results by Schlumberger arrangements, while open circles by bipole-bipole arrangements. A, B and C represent apparent resistivities obtained by the pairs of electrodes, A, B, and C as illustrated in Fig. 1.

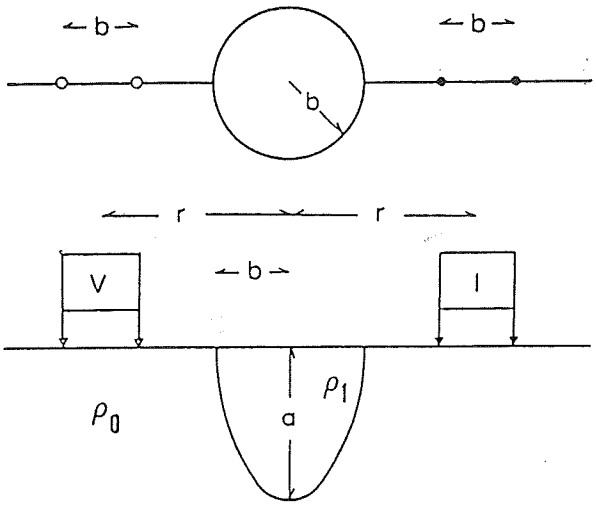

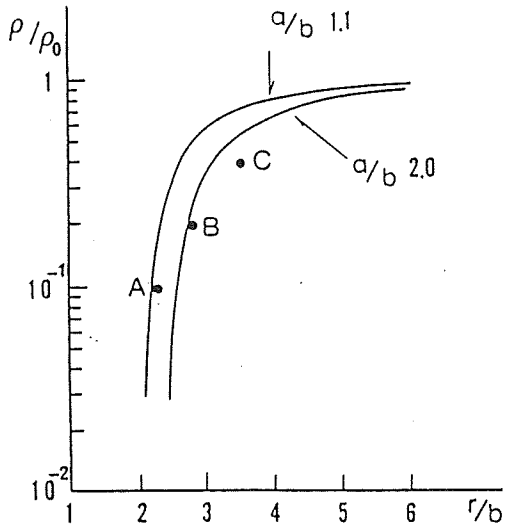

Fig. 3 Apparent resistivity curves for the ellipsoidal crater model.

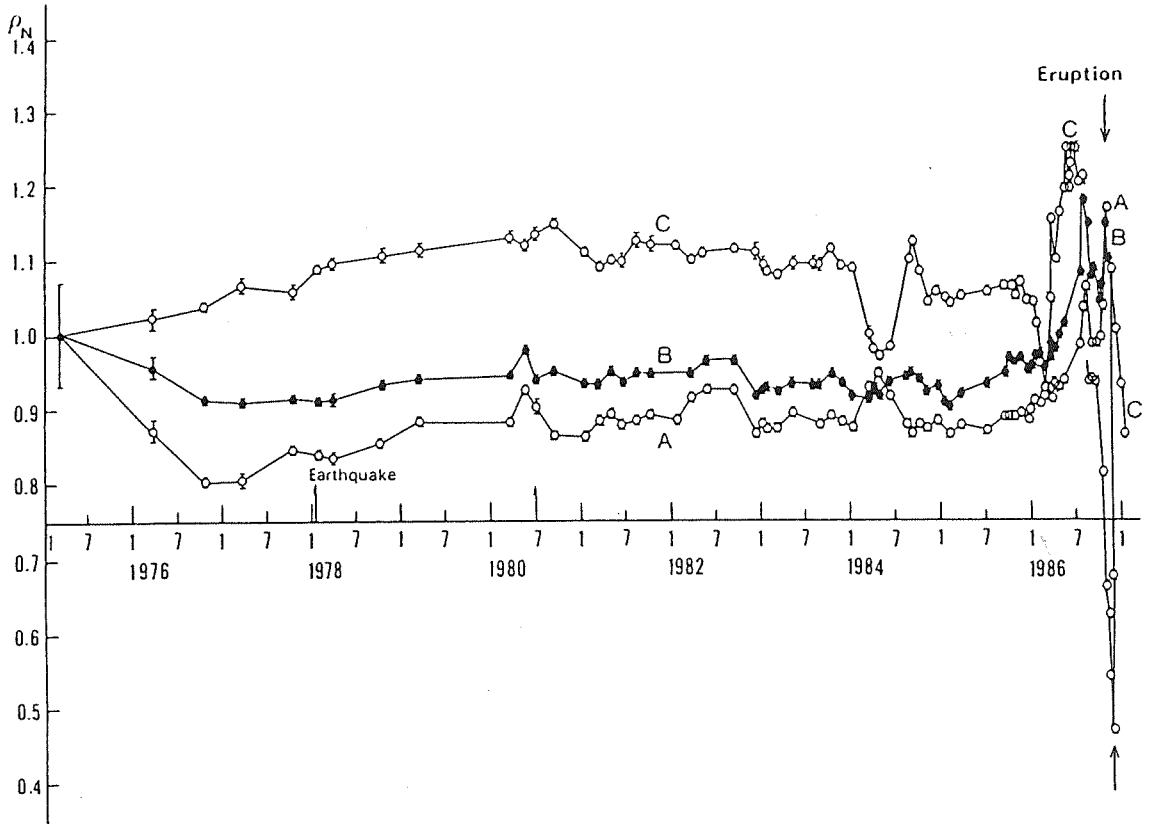

Fig. 4 Time variations in the apparent resistivity obtained by measurements across the central crater, Mihara-yama, with the electrode arrangements illustrated in Fig. 1.

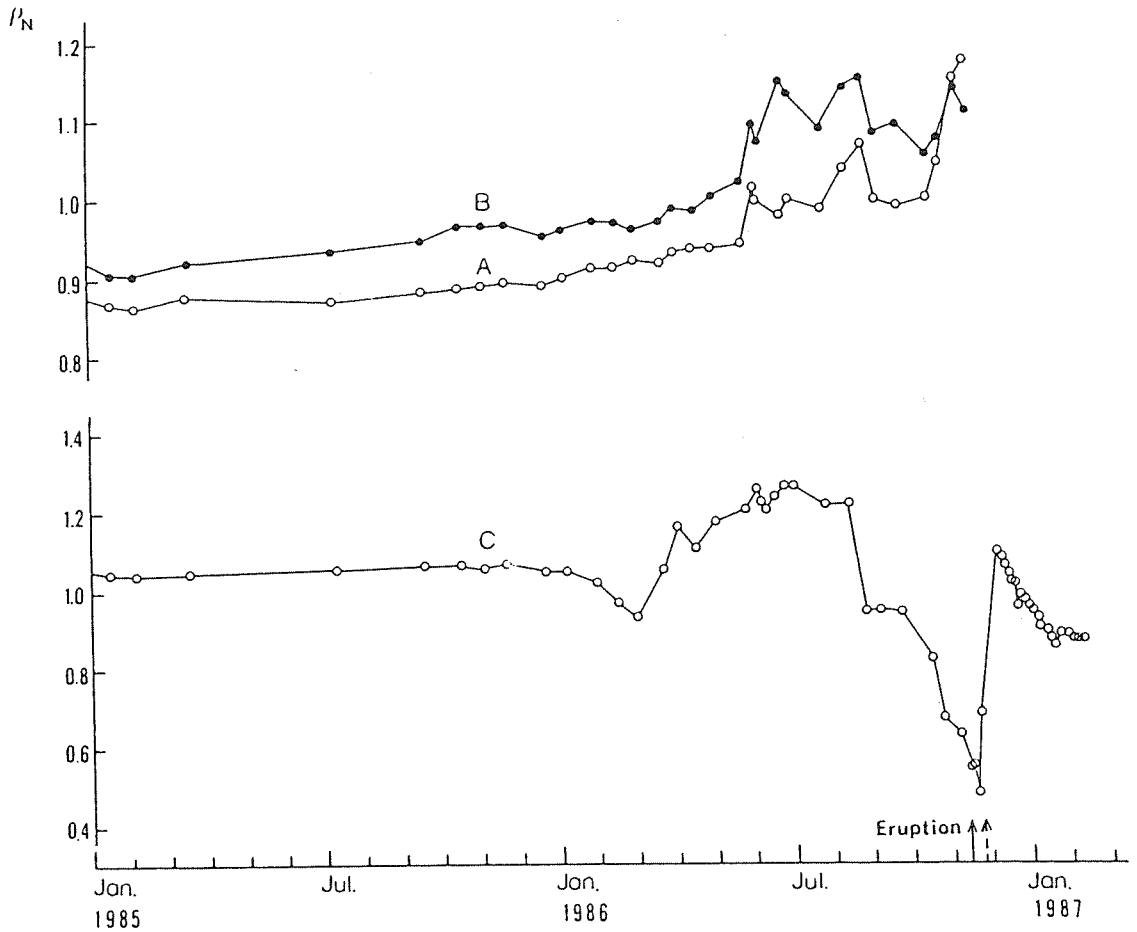

Fig. 5 Details of variations in the apparent resistivity.

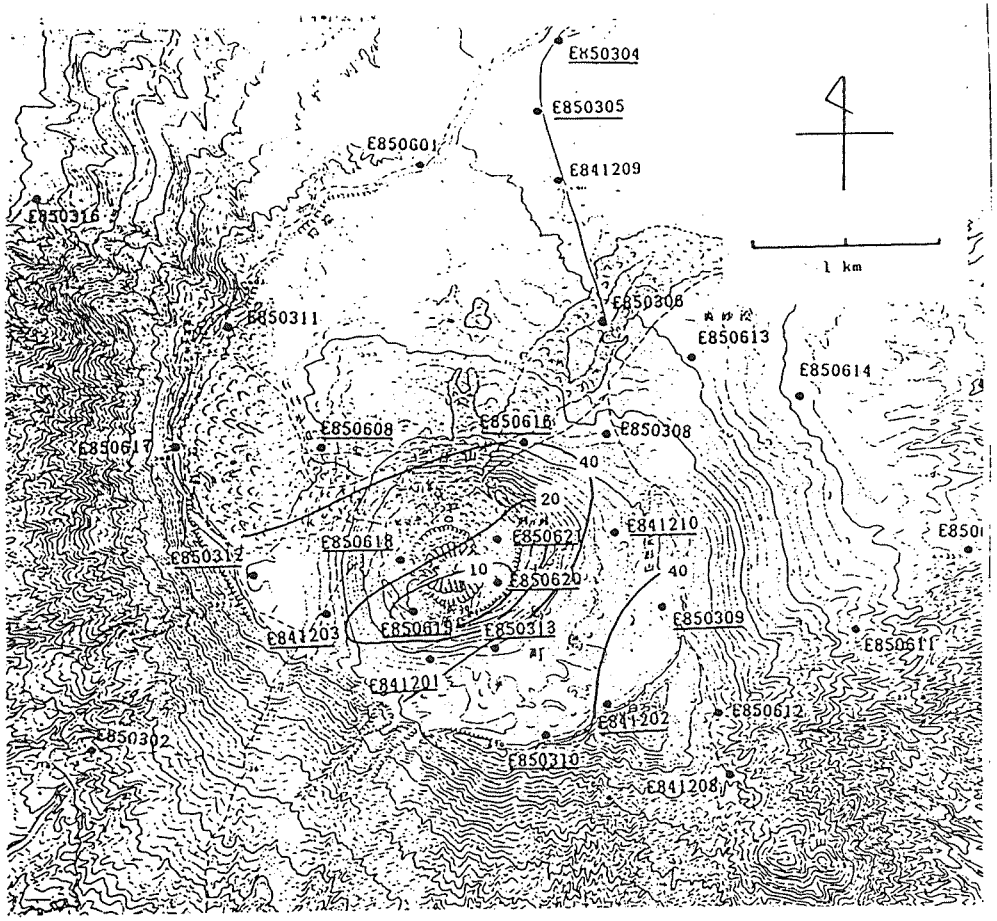

Fig. 6 Distribution of apparent resistivity obtained by electromagnetic induction method for 8 Hz in October 1986.

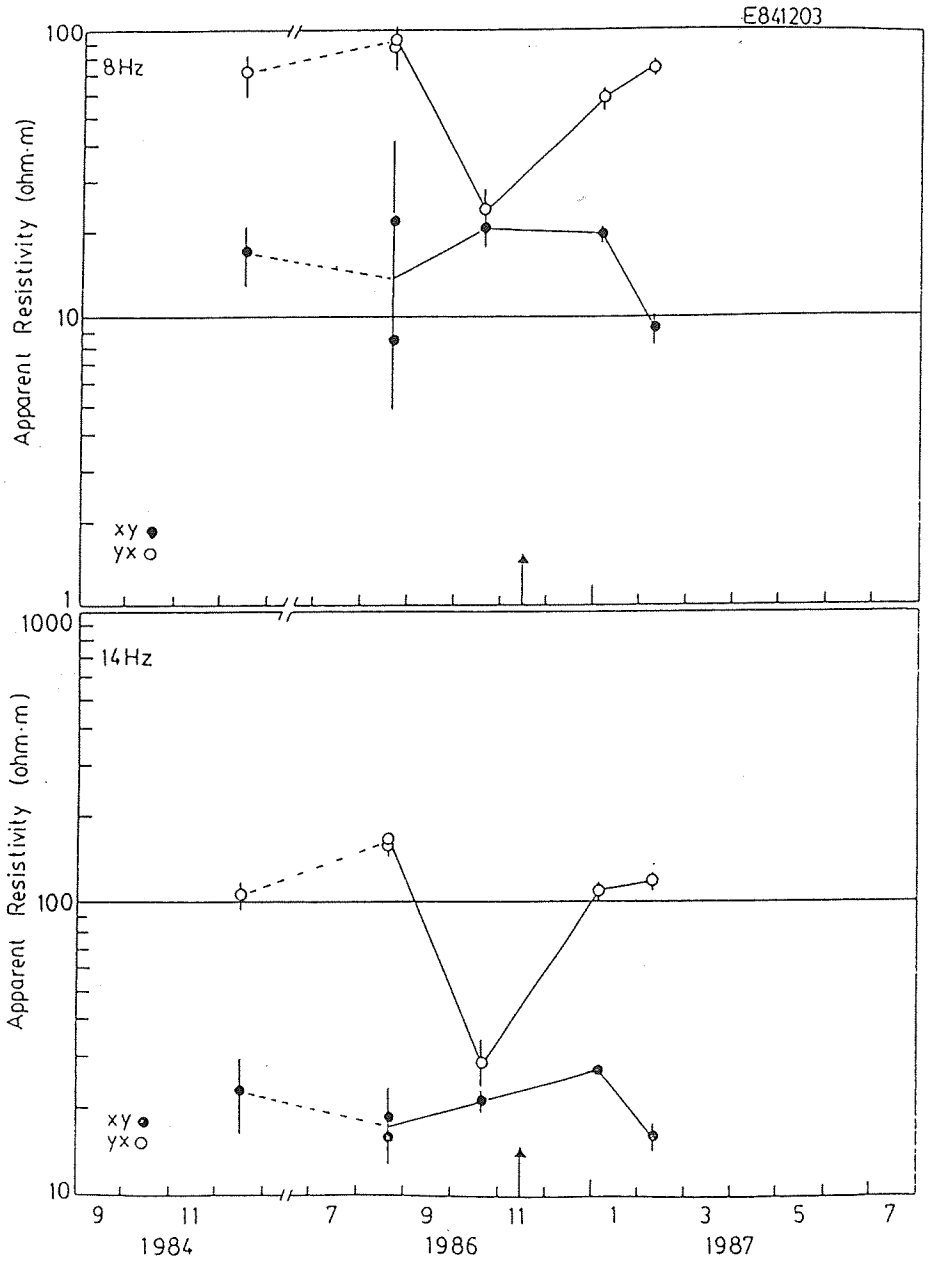

Fig. 7 Time variation in apparent resistivity at site E841203 for 8 and 14 Hz.

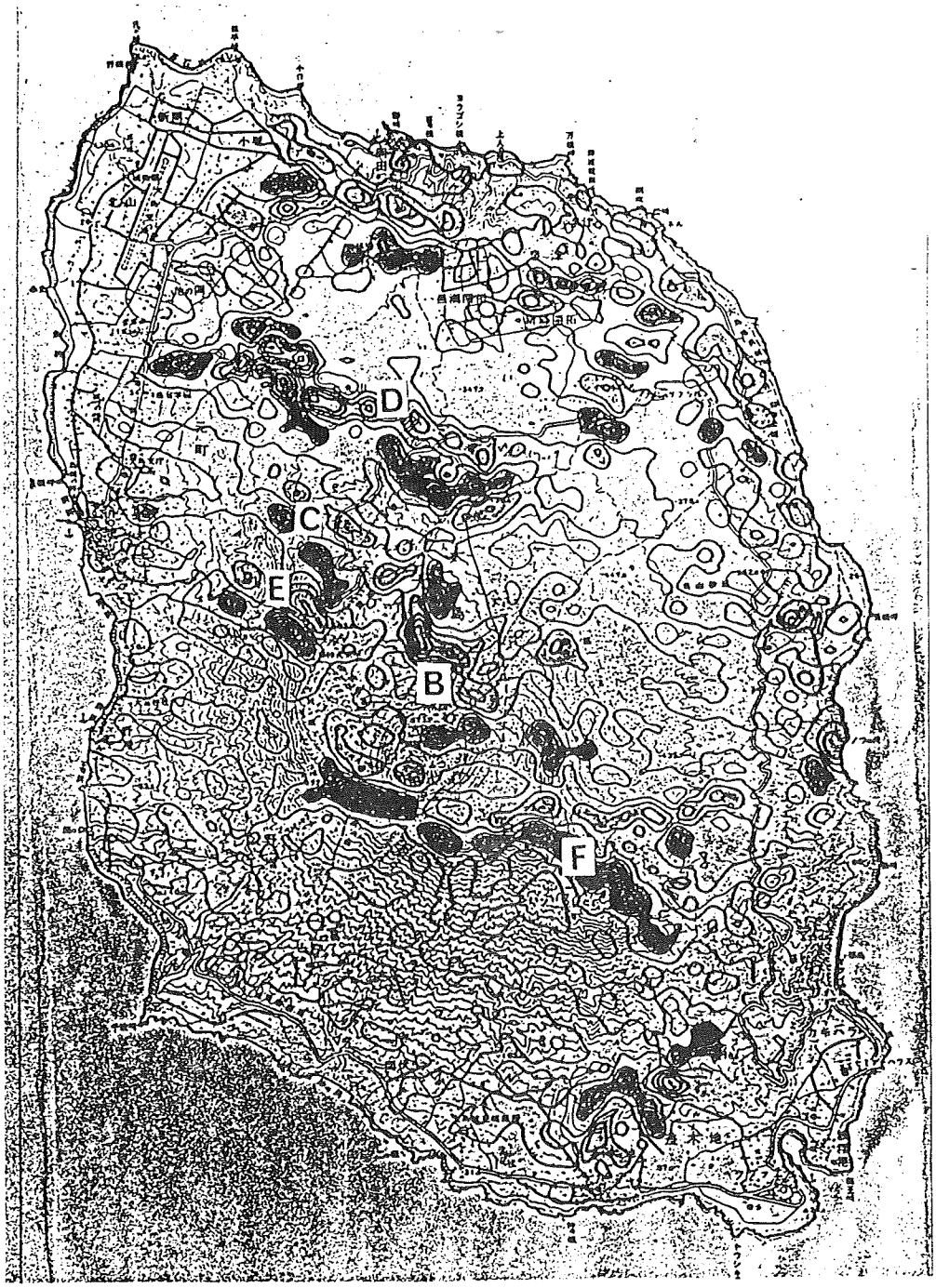

Fig. 8 Anomaly map for the gradient of Z/H for 17.4 kHz. Dark shade represents negative gradient, light shade positive gradient.